Feeding and growth of a dyke-laccolith system (Elba Island, Italy) from AMS and mineral fabric data

Emanuele Roni[a], David Scott Westerman[b], Andrea Dini[c], Carl Stevenson[d], Sergio Rocchi[a]*

[d] *Dipartimento di Scienze della Terra, Università di Pisa (Italy)*
[b] *Geology and Environmental Science, Norwich University (Vermont, USA)*
[c] *Istituto di Geoscienze e Georisorse, CNR, Pisa (Italy)*
[d] *School of Geography, Earth and Environmental Sciences, University of Birmingham (UK)*
* Corresponding author, email: rocchi@dst.unipi.it

Abstract: Dykes feed laccoliths and sills, however the link between feeder and intrusion is rarely observed. The felsic San Martino laccolith displays a clear feeder-intrusion link, allowing reconstruction of the influence of the size and location of feeder dykes on magma flow during formation of sub-horizontal intrusions. This work uses anisotropy of magnetic susceptibility (AMS) combined with mineral shape-preferred orientations of sanidine megacrysts to examine magma flow pathways through feeders into a laccolith. Strong correlation between AMS and K-feldspar data sets indicates that alteration affecting the paramagnetic mineralogy did not influence AMS results. The well established field relationships between feeder and laccolith provided a robust "geo-logical" model for flow pathways that we have used as a framework to aid interpretation of AMS data. The position and size of the main feeder dyke helped to predict the flow paths in the overlying laccolith. Our results show that magma spread laterally from the feeding system and built the laccolith layers with propagating and inflating divergent flow where tabular particles became aligned perpendicular to the magma displacement direction. The lack of internal discontinuities indicates that the magma was injected as a single pulse or a series of quickly coalescing pulses.

Supplementary material: AMS methods, AMS data and detailed fabric maps are available at http://www.geolsoc.org.uk/SUP0000.

Shallow igneous intrusions record the link between plutonic and volcanic processes. In particular, models of magma supply, accommodation and storage in intrusive bodies contribute to explain the evolution of felsic magma chambers (Miller & Miller 2002; Bachmann *et al.* 2007; Bachmann & Bergantz 2008). Recent multidisciplinary studies have led to the widely held view that igneous bodies often grow by incremental thickening/inflation of initially thin, sheet-like or tabular bodies by the addition of successive magma pulses (McCaffrey & Petford 1997; Cruden & McCaffrey 2001; Saint-Blanquat *et al.* 2001; Rocchi *et al.* 2002; Menand 2008), overlapping of sub-horizontal sheets (Horsman *et al.* 2005; Saint-Blanquat *et al.* 2006; Morgan *et al.* 2008) or amalgamation of magma fingers and tongue-like lobes (Stevenson *et al.* 2007). Incremental magma intrusion is also a common interpretation of geophysical observations of deformation episodes at active volcanoes (Biggs *et al.* 2011).
This study contributes to understanding magma flow during feeding and growth of shallow-level intrusions (< 3-4 km deep) by investigating their internal structures. However, rock fabrics can be difficult to disentangle for several reasons. First, the final rock

fabric may result from "pure" magmatic processes (e.g., emplacement flow, convection), late magmatic processes (thermal contraction, gravitational compaction) or tectonic processes (syn-emplacement deformation, post-emplacement deformation), or a multiple overprinting of them all. Second, magmatic fabric reflects finite strain produced by progressive magmatic flow rather than directly recording a simple flow direction (Saint-Blanquat *et al.* 2006; Paterson *et al.* 1998).

We therefore performed a multidisciplinary analysis: relevant data are represented by field observations, structural measurements of mineral foliations and lineations, and a large collection of anisotropy of magnetic susceptibility data (AMS). Additionally, this study focuses on fabrics in both a laccolith system and its feeder dykes, hence these data constrain the movement of magma in feeders as well as in the main sites of accumulation.

Here we use the late Miocene San Martino felsic laccolith, Elba Island, Italy, as a case study. Its geometry and emplacement/tectonic history are well defined (Dini *et al.* 2002; Rocchi *et al.* 2002; Westerman *et al.* 2004; Dini *et al.* 2006; Rocchi *et al.* 2010), thanks in part to serendipitous tectonic tilting that exposed several transects of the laccolith layers from top to bottom. This igneous body offers the chance to study internal structures that are undoubtedly magmatic since it crystallized very quickly, experienced no detectable subsequent ductile deformation, and local brittle tectonics (sliding and tilting of the laccolithic complex as a single rigid body) did not affect internal structures. Geometric data for the San Martino laccolith led to infer a two-stage growth model, with initial expansion of a thin sill followed by a vertical inflation stage (Rocchi *et al.* 2002). Our new fabric data allows the reconstruction of internal structures and presents a more refined picture of magma emplacement during laccolith growth.

Geological framework

The Setting

The Elba Island region was involved during late Cretaceous-early Miocene in the convergence-collision process between the Sardinia-Corsica block and Adria plate. This process resulted, on Elba Island, in a stack of thrust complexes (Fig. 1) (Bortolotti *et al.* 2001). Collision was followed by extensional processes coupled with eastward-propagating emplacement of igneous complexes (Serri *et al.* 1993; Serri *et al.* 2001). Between ~8.5 and 5.8 Ma, the two uppermost thrust complexes (comprised of a Jurassic ophiolite sequence with its cover, and a Cretaceous-Eocene turbidite unit) were intruded by laccoliths, plutons and dykes. In western-central Elba the igneous sequence started with the emplacement of the two-layers Capo Bianco aplite (~8.5 Ma) (Maineri *et al.* 2003; Dini *et al.* 2007). These layers were intruded and fragmented by the four intrusive layers of the felsic, sanidine-phyric Portoferraio porphyry (7.95 Ma) (Dini *et al.* 2002). Then, intrusion of the felsic, sanidine-megacrystic San Martino porphyry followed (7.4 Ma) (Dini *et al.* 2002). Altogether, these intrusions are defined as multilayer laccoliths (Rocchi *et al.* 2002) based on the overall parallelism of intrusive contacts and host rock anisotropies (Fig. 2c), tapering of visible terminations, and upward-convex roofs and flat to upward-convex floors (Dini *et al.* 2006). The layers of each intrusive unit are connected by dykes (Fig. 2d), generating an overall geometry typical of a nested Christmas-tree laccolith complex (Corry 1988). Magma was emplaced at a depth between 1.9 and 3.7 km, mostly along planar anisotropies such as thrust surfaces between tectonic complexes, secondary thrusts inside complexes, and bedding within the turbidite sequence.

Emplacement of the laccoliths was followed by intrusion of the ~2.5 km-thick monzogranitic Monte Capanne pluton (7 Ma) (Dini *et al.* 2002; Farina *et al.* 2010) and the Orano mafic dyke swarm (6.95 Ma) (Dini *et al.* 2008). The laccolith complex, originally intruded in the present western Elba area, was translated eastwards along with country rock by gravitationally driven tectonic collapse along the Central Elba Fault (Fig. 1). The lower section is now exposed in western Elba while the upper resides in central Elba (Trevisan 1950; Pertusati *et al.* 1993; Daniel & Jolivet 1995; Westerman *et al.* 2004). Following this eastward translation, west-side-up normal movement occurred along the Eastern Border Fault with a throw of 2-3 km near the margin of the pluton.

The San Martino Laccolith System

The laccolith consists of porphyritic rock, with prominent euhedral sanidine megacrysts set in a very fine-grained groundmass (<100 µm; Fig. 2a, b). Megacrysts are dominantly tabular on (010) and elongated on the *c* axis; minor prismatic crystals elongated on *a* are also present. Megacryst abundance is 50-200 crystals/m^2 with an average size of 5x2x1 cm (max 14x6x3 cm), corresponding to 3-12 vol%. Phenocrysts also include quartz (1-20 mm), plagioclase (1-5 mm) and biotite (1-5 mm). Groundmass consists of an equigranular, isotropic aggregate of quartz and feldspars, along with accessory apatite, zircon and monazite. Weathering and hydrothermal alteration are widespread, with replacement of plagioclase by calcite+sericite, sanidine by sericite, and biotite by chlorite, plus additional formation of titanite, anatase and/or rutile, and scattered late-magmatic tourmaline spots.

The San Martino laccolith is composed of three main, westward-dipping subparallel layers cropping out in central Elba, as well as several dykes in central Elba below the laccolithic layers and in western Elba as the roots of the original laccolith complex left behind after its eastward translation (Fig. 1). The emplacement level for this unit is as shallow as ~2 km (Rocchi *et al.* 2002). Contact metamorphic effects in the host rock are practically absent. The filling time of the 21 km^3 intrusion has been estimated around 100 years, based on the size of the dykes in western Elba and assuming a conservative ascent rate of 3×10^{-3} ms^{-1} (Rocchi *et al.* 2002). Internal magmatic layering and/or contacts are not observed.

Layer 1 is topmost and most voluminous, reaching a thickness of ~700 m (tapering toward both the northern and southern ends) with a N-S length of 8.3 km (Fig 3). It is characterized by branching patterns toward its margins. A prominent southern branch on the west shore of Marina di Campo Bay exposes a ~250 m thick bottom-top section that trends N-S and dips 30° W. Its base is marked at the south end by a gently west-dipping, ~300 m thick cross-section at Punta Mele; at the north end the base is well exposed at La Biodola Bay as a ~500 m thick bottom-top section. Layer 2 represents less than 5% of the total laccolith volume, striking NW-SE for about 1 km in the northern half of the complex. Its thickness decreases from ~150 to ~100 m from south to north. The lowermost Layer 3 parallels Layer 2 with an exposure length of 2 km and a thickness of ~250 m.

Six steeply dipping dykes of San Martino porphyry are mapped in western Elba (Fig. 1). The largest, the WNW-ESE Marciana dyke 1500 m long and 10 to 20 m thick, is interpreted as the main feeder (Rocchi *et al.* 2002). In central Elba, the subvertical NE-SW oriented Sansone dyke is the most significant, exposed over 400-500 m with widths of 3-20 m. Its structural location below the laccolith (Figs. 1 and 2d) suggests it locally fed Layer 3.

With the aim of describing and interpreting the fabric data in their original geometric context, i.e. before eastward translation and rotation (Fig. 1) (Westerman *et al.* 2004), all central Elba data has been rotated west-side-up by 30° around a N-S horizontal axis. Data discussed in the text, therefore, refers to a body having sub-horizontal basal contacts and slightly upward convex tops, with steeply-dipping dykes below.

Fabric results

Two approaches were taken to establish the igneous fabric within the San Martino laccolith complex: direct determination by measuring the orientation of sanidine megacrysts (Fig. 3a), and indirect determination by measuring anisotropy of magnetic susceptibility (AMS) parameters (Fig. 3b). The use of multiple independent fabric determinations is of fundamental importance in validating fabric analysis.

Megacryst fabric

Shape-preferred orientations of sanidine megacrysts have been measured using (010) faces of tabular crystals, while magmatic lineations were determined using the *c* axes of elongated/tabular crystals or the *a* axes of prism-like crystals elongated on *a*. Tabular crystals with weak elongation yielded only foliation data. These crystallographic features are best recognized where crystals show 3D exposures (Fig. 2a, b), such as along weathered shorelines cliffs. Statistically controlled foliation values were determined at 48 stations and lineation at 36 stations, with both values measured at 34 of those sites (Table 1S). Foliation measurements were made on 25 to 99 contiguous crystals at each station, while lineation measurements derived from 30 to 97 crystals. Foliation measurements based on average crystal patterns were made at an additional 19 sites.

Throughout the laccolith system, the investigation of megacryst attitudes points out well-defined magmatic foliations along with weak magmatic lineations. In fact, foliation poles in 85% of the stations (41/48) have the main eigenvalue (E1) > 0.6 and almost 60% (28/48) have E1 > 0.7. In contrast, magmatic lineations in 50% of the stations have the main eigenvalue > 0.6 and in only the 13% (5/36) have E1 > 0.7 (Table 1S).

Taken together, magmatic foliations within Layer 1 (Fig. 3a) show distinctive patterns that change progressively, emanating from the west-central part of the layer where a distinct N-S striking foliation has been measured. This N-S attitude continues to the east, but foliation attitudes rotate clockwise toward the south and anticlockwise toward the north. In the southern part of this layer, foliations rotate progressively to a NE-SW attitude, then to E-W, and finally to NW-SE at the south-westernmost exposures. A detailed study at the southern edge of Layer 1 ("Casa Ischia"; Fig. 2S) shows changes in orientation from NW-SE in the lower portions, to N-S in the central part, to NE-SW in the upper portion, all with variable dips. In the northern part, the rotation shows a mirrored pattern, progressing through a widespread NW-SE orientation, to E-W attitudes along the northernmost margin of the layer. A second detailed study of sanidine megacryst fabric in the north ("Lamaia sheet"; Fig. 3S) reveals homogeneous fabric from bottom to the top. Dips of foliation throughout Layer 1 are highly variable with no clear spatial patterns.

Two lower laccolith sheets are exposed in the northern part of the system. Layer 2 has a dominant fabric with foliation and lineation trending predominantly NE-SW, while fabric in Layer 3 is generally NW-SE for much of the unit but transitions anticlockwise through E-W toward the NW terminus of the laccolith. Lineations are distributed at various attitudes, within the plane of foliation and, more commonly than not, either close to strike or running down dip. Where observed, sanidine foliation in both the Sansone and Marciana dykes are sub-parallel to the steeply inclined dyke walls.

Magnetic parameters

The second approach to determining the internal fabric of the San Martino laccolith was to determine anisotropy of magnetic susceptibility (AMS) parameters, which is controlled by the orientation of crystals of the mineral(s) dominating the magnetic signal. AMS is a technique that gives a quantitative description of the crystalline fabric of a rock by determining the variation of magnetic susceptibility with direction such that the eigenvector K_1 represents the magnetic lineation while K_3 is the pole of the magnetic foliation (Tarling & Hrouda 1993; O'Driscoll *et al.* 2008).
We sampled 150 sites in the laccolith horizons and their feeder dykes (Fig. 4S). In addition, clusters of samples were collected at selected locations to investigate the distribution of magnetic parameters at a very local scale (e.g., thin branches of the layers, outer and inner parts of dykes). The relationship between the mineral preferred orientation and magnetic fabric depends on the nature of the magnetic mineralogy, here represented by biotite, with rare tourmaline and very minor Ti-rich oxides. Biotite is commonly chloritised, but no significant formation of Fe-oxides is also supported by: (1) low measured susceptibilities ($1.9 \times 10^{-4} \div 2.2 \times 10^{-5}$ SI units), typical of rocks characterized by paramagnetic mineralogy (Tarling & Hrouda 1993); (2) K_m for altered/weathered samples similar to K_m of the freshest rocks (Table 2S); (3) heating/cooling experiments on fresh, chloritised, and chloritised/weathered samples all showing an overall paramagnetic behaviour (Fig. 4).

Magnetic fabric in dykes

Data for all the dykes indicate that both the shape parameter T and the anisotropy degree P_j are quite variable (Fig. 5). Site mean values of T vary from -0.554 to 0.918 while P_j values are general low (1.009 to 1.129). The map of the Marciana dyke in western Elba (Fig. 6) suggests an overall parallelism between magnetic fabric and dyke walls. The perpendicularity of the best-fit great circles of lineations and poles to foliation confirms that K_1 (lineation) lies within the plane of foliation. Detailed fabric analysis shows local "normal" fabric (Rochette *et al.* 1992) with K_3 sub-orthogonal and K_1 sub-parallel to the outer walls; fabric close to the walls shows upward-SE imbrication in both horizontal and vertical sections. Lineations near dyke walls are generally oblique with imbrication plunging toward the walls; interior lineations are sub-horizontal. Elsewhere, strong fabric asymmetry occurs with no reversal of imbrication across the dyke. Magnetic foliation and lineation in the Sansone dyke in central Elba (Fig. 6) commonly parallel the overall N55E strike of the dyke, with dips less steep than dyke walls.

Magnetic fabric in the main laccolith body

In the main laccolith body, the shape parameter T ranges from -0.836 to 0.891 (Fig. 5; Table 2S). Data from the middle and lower parts the laccolith reveals oblate range of ellipsoid shapes, while shapes for the upper part are predominantly oblate, illustrating that fabrics are dominated by foliation (flattening) rather than lineation (constriction). The T

parameter is highly variable at both the laccolith and local scale. Values of the degree of anisotropy (P_j) in the laccolith are fairly low, ranging from 1.006 to 1.081 (Fig. 5) as is typical in granitic rocks (Horsman *et al.* 2005). The use of AMS allowed recognition of a well-defined magnetic fabric that is almost everywhere quite strong: 86% of the samples (129/150) have $e_3 < 25°$ while 75% of the samples (113/150) have $e_1 < 25°$, where e1 and e3 are the semi-angles (measured in degrees) of the confidence ellipses around the mean-value of K_1 (magnetic lineation) and K_3 (pole of magnetic foliation). Only 6% of the samples (9/150) have both e_1 and $e_3 > 25°$.
Magnetic fabrics (Fig. 3b) are decidedly similar to those revealed by sanidine megacryst analyses (Fig. 3a), with clockwise rotation of AMS fabric in Layer 1S, mirrored by an anticlockwise rotation in Layer 1N. Detailed study at Casa Ischia on the southern coast (cross-section southern termination of the main body; Fig. 2S) shows the same progressive bottom to top changes described above for magmatic fabric. The lowermost 100 m has magnetic foliations striking NNW-SSE with dips 35-70° NE, while foliations in the uppermost 150 m strike NE-SW and dip variably. Results of a similar detailed study in the Lamaia sheet on the north shore (Fig. 3S) show E-W strikes of magnetic foliation like their sanidine counterparts, but dips increase progressively from <30° at the base, to 30-60° in the core, to sub-vertical near the upper contact. Data for Layer 2 show consistently NE-SW-striking foliation, with gentle SE dips at the southern termination and steep dips further north. In the lowermost Layer 3 the foliation has NW-SE mean strike with variable dip.

Discussion

Correlation of AMS and megacryst fabric data

AMS fabric data and shape-preferred orientations of sanidine megacrysts, along with structural reconstructions, allow development of an internally consistent model of magma flow and laccolith growth. Before presenting the model, some concerns will be addressed. First, some recent work suggests caution in interpreting flow structures in intrusive rocks, owing to possible subsolidus development of phenocryst-bearing texture in cases of thermal cycling (Mills *et al.* 2011). However, this doesn't apply to the San Martino laccolith, which suffered unidirectional quick cooling as supported by the sanidine structure of its K-feldspar megacrysts.
Secondly, many previous studies did illustrate how AMS can be used successfully to determine magmatic fabric patterns by direct correlation between fabrics from mineral shape-preferred measurements and AMS fabrics (Bouillin *et al.* 1993; Saint-Blanquat *et al.* 2001; Saint-Blanquat *et al.* 2006; Horsman *et al.* 2005; Guillet *et al.* 1983; Darrozes *et al.* 1994). Nevertheless, we tested the correlation of igneous foliation preserved by sanidine megacryst attitudes and that of biotite as revealed by AMS for the San Martino laccolith. Results from 25 sites where both AMS and detailed megacryst fabric data were collected reveal general concordance (Table 1): the angle between magnetic foliation and the megacryst foliation is <30° in 16/25 (65%) stations and the angle between magnetic and megacryst lineation is <30° in 6/7 (85%) stations. Given that highly oblate biotite crystals generate the AMS fabric, the observed parallelism of tabular sanidine and AMS fabrics indicates that both crystal sets recorded similar strains (magmatic flow).
Correlations between lineations derived from the two methods are not so easily explained, since the AMS lineation comes from biotite crystals, that are not elongated. We conclude

that the K_1 lineation is most likely due to the platy biotite crystals being preferentially oriented along a "zone axis" within the plane of mineral foliation (Bouchez 1997). This requires that the highly oblate biotite wobble within the plane of foliation, and also that this line be coincident with the line along which elongated sanidine crystals trend, most probably corresponding to the axis of maximum stretching during magma flow.

Relation of magmatic fabric to magma flow

Having established that AMS fabric in the San Martino system mimics megacryst attitudes, the next assessment concerns how such petrofabric data can preserve evidence of magma flow paths. This is problematic since (i) fabric can result from multiple events (flow, tectonic deformation, hydrothermal activity, etc.), and (ii) fabric reflects finite strain generated by differential stress due to progressive magmatic flow (Paterson *et al.* 1998).
Based on the absence of appreciable signs of solid-state deformation, an overprint of igneous AMS fabrics by regional deformation can be ruled out, even though the post emplacement history included tectonic translation from western to central Elba. Additionally, regularly varying patterns of fabric within the intrusions show that stresses were local and, therefore, not a record of regional paleostress. Other processes able to impart a fabric, such as filter pressing or porous flow, are also unrealistic in this case due to the low percentage and homogeneous distribution of phenocrysts in the magma during emplacement flow. Additionally, this laccolith was emplaced rapidly (Rocchi *et al.* 2002) and was quickly solidified (very fine-grained matrix). We can thus infer that the observed fabrics reflect the final increments of strain as the magma was moving and solidifying.
The lack of magmatic layering, internal magmatic contacts and/or internal shear zones in the laccolith suggests that the magma was injected to form the different layers as either a single pulse or as batches coalescing shortly after or during injection. In the latter hypothesis, the time gap between pulses had to be shorter than the solidification time of the preceding pulse. While this thermal requirement is more feasible for slowly cooling, deep-seated igneous bodies (Farina *et al.* 2010), there are examples of such processes in shallower, but more mafic, igneous bodies (depth ~2.5 km) such as the Black Mesa intrusion (Saint-Blanquat *et al.* 2006). These constraints suggest that our fabric markers formed during the waning stages of a single episode of flow: the fabric represents only the strain occurring in the final stages of emplacement making it difficult to test the two-stage (horizontal spreading then vertical inflation) model for this system (Rocchi *et al.* 2002).
Given these conditions, it is fundamental to define which fabrics can be generated by the different types of magmatic flow (Paterson *et al.* 1998). If magma flows in any way other than with a uniform velocity field, such that crystals are not forced to rotate to a preferred orientation, then a stress field will be produced that will orient tabular and linear crystals. Tabular crystals become oriented perpendicular to the direction of maximum shortening and linear crystals get aligned parallel to the direction of maximum stretching. Three end-members of non-uniform flow may be considered here: (i) convergent flow, occurring when magma moves to a progressively narrowing region with associated velocity increase; crystals align their longest axes and largest crystal faces with the particle path; (ii) divergent flow, occurring when magma spreads in progressively widening regions with divergence of flow lines and velocity decrease; planar fabrics develop in the plane of flattening perpendicular to particle paths, while lineation develops in the flattening plane, parallel to the stretching direction; (iii) non-coaxial flow, generated by drag along a

boundary surface affected by simple shear, with velocity increasing away from a boundary surface; fabric forms a variable angle with that surface.

All of these may be present over short distances to define units of flow where non-coaxial flow is combined with either convergent or divergent flow, as in flow lobes (Stevenson *et al.* 2007). Nevertheless, laccolith emplacement is characterised by lateral spreading and filling, with the cross-sectional area of the feeding system remaining quite constant (i.e. a feeder dyke) while the cross-sectional area of the laccolith grows. Such conditions would make divergent flow the norm within filling laccoliths. Transitions in fabric-flow relationships have been documented in experiments (Kratinová *et al.* 2006) where magnetic fabric inside the feeder (i.e. constricted) was parallel to the transport direction of the "magma", but further away (i.e. diverging), the fabric rotated by 90° to become perpendicular to the transport direction. On the other hand, in thin dykes where all the magma is relatively close to the walls, non-coaxial flow generates an imbricated foliation along dyke walls. Similarly, in sub-horizontal sheets, where the centre of each igneous sheet flowed more rapidly than the edges (Correa-Gomes *et al.* 2001; Gil-Imaz *et al.* 2006), symmetrical imbrication of foliation planes develops at the upper and lower contacts (Komar 1972, 1976), as shown also by analog modelling (Kratinová *et al.* 2006).

This discussion on fabric-flow relationships relates to the issue that published papers commonly present a seamless transition between maps showing shape-preferred orientation and/or AMS fabrics, and maps or diagrams presenting the magma flow history as deduced from the fabrics. However, a variety of fabric-flow relationships are used in interpreting these fabric data, according to the different types of inferred magma flow.

Magma flow in feeder dykes

Magma flow in dykes has traditionally been inferred with the assumption that K_1 is oriented parallel to the direction of magma flow (Rochette *et al.* 1991), with the sense of flow determined using the symmetrical imbrication of K_1 (Knight & Walker 1988). However, magnetic lineation can be perpendicular to magma flow (Rochette *et al.* 1999; Rochette *et al.* 1991; Dragoni *et al.* 1997) and the intersection of magnetic foliations can result in an apparent magnetic lineation (Callot & Guichet 2003). For these reasons some authors (Geoffroy *et al.* 2002) established that imbrication of magnetic foliation better constrains magma flow direction than does simple magnetic lineation.

Flow histories for the Marciana and Sansone dykes have been interpreted from both AMS and sanidine petrofabric data, using the theoretical and empirical bases noted above. Investigation of internal structures has mainly focused on interpretation of the attitudes of foliation due to the planar and oblate nature of the magnetic carrier (biotite), along with the tabular shape of most sanidine megacrysts (Fig. 6). Marciana dyke in western Elba lies beneath the former location of the San Martino laccolith. The sub-vertical fabric, general parallelism, and imbricated orientation of AMS foliation and lineation near the dyke walls, combined with moderately inclined foliations (and lineations) in the dyke core with respect to the walls, suggests that the dominant magma flow was sub-vertical. Fabrics in the Sansone dyke at the base of the laccolith in central Elba are also suggestive of vertical magma flow, in that foliation is typically subparallel and imbricated with respect to dyke walls, while lineation is generally steeper near the dyke walls than in the core.

Magma flow in laccolith horizons

When an intrusion grows in two stages, such as a sill inflating to a laccolith as Papoose Flat, the relationships between fabric and magma flow also evolve through time (Saint-Blanquat *et al.* 2001). A foliation parallel to the sill shape develops during the sill formation stage. During inflation and transition to laccolith shape, when flow is mainly vertical, foliation develops perpendicular to flow, retaining the pattern with foliation parallel the upper contact in the core of the body away from the solid-state fabric. Lineations close to the contact (<1 m) are parallel to flow due to wall rock interaction and shear, while below that, lineations are parallel to the stretching direction perpendicular to flow. The case of magma flowing in lobes is illustrated by the Trawenagh Bay granite, where AMS fabric data define frozen lobes of granitic magma (Stevenson *et al.* 2007). Foliations are aligned parallel to the lateral margins of the lobes and wrap concentrically around lobe noses, while lineations trend parallel to the elongation of lobes. In thin sills with fingers, like in the Henry Mountains, magnetic foliation trends sub-parallel to contacts with lineations presenting a radiating pattern in the fingers off the main body of the sill (Horsman *et al.* 2005). In a nearby small, flat pluton, strong parallelism of concentrically arranged foliations from both AMS and field fabric data is reported (Saint-Blanquat *et al.* 2006).

These interpretations of flow history seem entirely plausible, yet the rules for getting from fabric to flow are not generally presented. The rules used appear to vary considerably, largely because the assumptions used to interpret flow patterns are not always clearly stated. Our approach to interpreting the San Martino flow history has been to start with the structural data (shape, geometry, location of feeders, etc.) and postulate a reasonable emplacement model to be tested using multiple fabric data sets and basic fabric-flow principles. We have thus far established that tabular and elongated sanidine megacrysts and biotite carrying the paramagnetic AMS signal have similar shape-preferred orientation that varies widely but in organized patterns. After considering available explanations for this coherence of fabric, we have concluded that crystal alignment recorded the strain produced by the stress field acting during the waning stages of magma flow.

The magnetic fabric is mainly oblate throughout the laccolith, probably linked to the dominance of flattening processes during the intrusion growth. Flattening in thick sheets is usually associated with divergent flow where particles align their largest faces orthogonal to flow directions. For this reason it has been assumed that the magma displacement direction (magma flow) in the laccolith layers was orthogonal to the foliation. On the basis of these considerations, AMS and megacryst fabric data can be used together to depict models for magma flow through feeder dykes and into the laccolith layers.

The Marciana dyke in western Elba is assumed to have been the primary feeder for the San Martino Christmas-tree laccolith system above, with smaller dykes serving as connectors between individual laccolith horizons. A schematic inset in Figure 7 (upper left) illustrates the diverging particle paths in magma spreading horizontally from a dyke with length less than the laccolith diameter. We assumed that flow within the sheets was away from the centrally located E-W feeding system. Given that the cross-sectional area of the feeder dyke was on the order of 0.2 km^2, while the horizontal area of the laccolith sheets reached 55 km^2 with multiple layers up to 700 m thick (Rocchi *et al.* 2002), divergent flow is assumed to have been the norm during laccolith growth. Figure 7 presents a map of interpreted flow directions assuming that flow was in the direction perpendicular to magmatic foliation (i.e. the plane of flattening), and parallel to the pole to such foliations. Note that foliation values on this map are corrected for subsequent tectonic rotation, while the map itself presents the current distribution of the laccolith sheets that dip 30° westward on average. Nevertheless, logical patterns develop when one assumes that poles to foliation preserve particle paths, and therefore, that foliation dips in the direction of upwardly inclined flow but dips away during downwardly inclined flow.

To interpret this map and the resulting emplacement model, we start along the western edge near the roof of the uppermost sheet of the system. Flow arrows plunge shallowly toward the east as a result of upward flow being directed eastward near the roof of the laccolith. Further east (and lower in the section), arrows diverge to show both northward and southward movement of the magma near the eastern termini of the sheet. Southern central Elba is dominated by southeastward flow, locally inclined upward, but predominantly plunging in the direction of flow. Flow paths have been confirmed in this area where strained quartz phenocrysts in the outer 1 cm skin of the sheet are aligned NW-SE parallel to the magmatic fabric measured several meters below.

Further to the south, flow rotates to predominantly due south, with local divergence. Detailed study near Casa Ischia (Fig. 2S) shows southward flow in the lowermost part of the sheet, with flow of the upper (western) part to the ESE. This sense is confirmed with strained quartz phenocrysts in the upper contact exhibiting differential flow. Magma below the skin flowed ESE to produce bookshelf structures of quartz, strained with aspect ratios up to 40. Further rotation of foliation at the south-westernmost exposures of San Martino porphyry indicates flow toward the SW. North of the central feeder system, flow patterns show particle paths reflecting northward movement of magma, with local divergence above and below a large septum of host flysch, and predominant flow toward the NE along much of the base of the uppermost San Martino sheet. Two smaller underlying sheets show general filling by NE-directed flow with divergence. Northernmost exposures, much like their mirror counterpart to the south, show the maximum rotation of flow off to the NW.

Figure 7 schematically presents the relationships between fabric, flow and position in the reconstructed laccolith system. Magma flowed sub-vertically within a central feeder dyke, as indicated by symmetrical imbrications of the sub-vertical AMS markers in sections orthogonal to the dyke plane. The dyke fed a laccolithic main body by lateral spreading of the magma, during which the oblate sanidine and biotite crystals became parallel to the plane of flattening that developed perpendicular to the magma displacement direction before the melt solidified to form the porphyry matrix. Reconstruction of reasonable patterns of filling for the laccolith horizons and the 3D patterns of flow within them was based on (i) correspondence of sanidine megacryst fabric and the biotite AMS fabric, and (ii) a model generated from detailed maps and reconstructions of the geology.

Implications

The possibility of interpreting all the megacryst and AMS fabric data in a unique frame of flow suggests that each laccolith layer grew in a single inflation episode. This inference implies that spreading and inflation were simultaneous as suggested on a theoretical basis (Michaut 2011), supporting laccolith emplacement as modelled by the elastic plate theory (Michaut 2011; Bunger & Cruden 2011). Alternatively, traces of the initial horizontally expanding sill are lost or yet to be documented, e.g. by collecting data along contacts where quenched magma shows deformation features compatible with extreme stretching.

Additionally, a fabric compatible with a single inflation episode could imply that (i) laccolith filling was by a single magma pulse, or alternatively, (ii) filling was by means of multiple, yet quickly coalescing pulses. Both possibilities agree with the short time scale inferred for laccolith formation based on the size of the feeding system (Rocchi *et al.* 2002), as well as on a theoretical basis (Michaut 2011). On the other hand, significantly longer times are suggested by calculating minimum filling rates for magma chambers (Annen 2011) or by dividing a laccolith volume by isotopically determined, highly resolved emplacement times (Michel *et al.* 2008). However, these timings have to be considered as averages, likely composed of emplacement bursts separated by intervals of inactivity (Cottam *et al.* 2010; Leuthold *et al.* 2012; Michel *et al.* 2008).

Conclusions

The strong correlation between megacryst and magnetic fabrics strengthens the use of AMS as a magma strain indicator. Furthermore, while megacrysts commonly give poor lineation data, AMS provides the magmatic lineation as a "zone axis".
Fabric (strain) in the rock and magma flow are closely related, thanks to fast emplacement and cooling, as well as to the lack of post-emplacement tectonic deformation. The magma feeding the laccolith layers flowed sub-vertically from a sizable central dyke. Magma then spread laterally as a single pulse or a series of pulses that quickly coalesced.

Acknowledgements This paper has been supported by Italy PRIN-2008PN8Z9K grant to SR and AD, and by funding from Norwich University (VT, USA) to DSW.

Figure Captions

Figure 1. Location map: **a)** Location of Elba Island, **b)** Geological map of Elba Island (Rocchi *et al.* 2010), **c)** Geological cross section illustrating the results of the tectonic history of Elba Island.

Figure 2. Images of San Martino porphyry: **a)** Typical outcrop with strong alignment of the megacrysts; **b)** Outcrop showing the typical size and shape of the megacrysts; **c)** Sill above the San Martino main sheet at the southern termination, Marina di Campo Bay; **d)** Sansone Dyke.

Figure 3. a) Restored sanidine magmatic fabric foliation data plotted on background geological map (Dini *et al.* 2006). Dip values as black numbers refer to detailed analyses; grey numbers indicate field estimates. **b)** Restored magnetic data showing magnetic foliation in red and magnetic lineation in blue. Numbers beside symbols are dip values. All measured values have been processed using Stereonet v.6.3.3 of R.W. Allmendiger (*http://www.geo.cornell.edu/geology/faculty/RWA/programs*).

Figure 4. a) Photomicrograph and **b)** SEM images of chloritised biotite. **c, d, e)** Results of heating experiments showing homogeneous decrease of susceptibility characteristic of paramagnetic minerals (biotite) during heating. Differences in paths of heating and cooling curves reflect oxidization during the heating with formation of maghemite. Susceptibility values are negative because the uniform influence of the sample-holder with a negative susceptibility of roughly -140 E-3 has not been removed. **c)** Fresh sample SLC3, with homogeneous decrease of susceptibility during heating (paramagnetic minerals) disturbed by a small bump at 570° (T° Curie of magnetite), suggesting a very minor ferromagnetic contribution; **d)** strongly chloritised sample ENF11; **e)** strongly weathered and chloritised sample BAR10.

Figure 5. T (shape anisotropy) vs. P_j (anisotropy degree) plot (Jelinek 1981) showing that flattening processes (positive T) are dominant, especially in the upper portions of the laccolith.

Figure 6. – **a)** Map of Marciana dyke in western Elba with strikes of K_1-K_2 planes (magnetic foliation) in red and trends of K_1 (magnetic lineation) in blue, measured at 19 sites including a complete transversal section. Owing to the variable strike of the dyke and to simplify reading of data, stereographic projections of foliations and lineations are plotted in relation to strike of the dyke rotated to E-W orientation for every site. The Marciana dyke remained in western Elba below the décollement surface of the Central Elba Fault, therefore these data have not been rotated for any tectonic restoration. **b)** Map of Sansone dyke with symbols as above, measured at 10 sites, with 3 complete transversal sections. Stereographic projections of magmatic foliations and lineations have been restored by 30° clockwise rotation around a horizontal N-S axis.

Figure 7. Magmatic flow pattern based on poles of restored magmatic and magnetic foliations projected on the current map pattern. Stereograms of foliations for Layer 1-

northern part, Layer 1-southern part, Layer 2 and Layer 3. Blue line trending E-W marks separation of N and S halves of Layer 1, with the west end representing the approximate eastern terminus of the Marciana feeder system. Upper left: conceptual model of fabric-flow relationships in the feeder dyke and a laccolith layer.

Table Captions

Table 1 - Angles between AMS data and megacryst measurements.

References

ANNEN, C. 2011. Implications of incremental emplacement of magma bodies for magma differentiation, thermal aureole dimensions and plutonism-volcanism relationships. *Tectonophysics,* 500, 3-10.

BACHMANN, O. & BERGANTZ, G. 2008. The magma reservoirs that feed supereruptions. *Elements,* 4, 17-21.

BACHMANN, O., MILLER, C. F. & DE SILVA, S. L. 2007. The volcanic-plutonic connection as a stage for understanding crustal magmatism. *Journal of Volcanology and Geothermal Research,* 167, 1-23.

BIGGS, J., BASTOW, I. D., KEIR, D. & LEWI, E. 2011. Pulses of deformation reveal frequently recurring shallow magmatic activity beneath the Main Ethiopian Rift. *Geochemistry, Geophysics, Geosystems,* 12, Q0AB10.

BORTOLOTTI, V., FAZZUOLI, M., PANDELI, E., PRINCIPI, G., BABBINI, A. & CORTI, S. 2001. Geology of central and eastern Elba Island, Italy. *Ofioliti,* 26, 97-150.

BOUCHEZ, J.-L. 1997. Granite is never isotropic: an introduction to AMS studies of granitic rocks. *In:* Bouchez, J.-L., *et al.* (eds.) *Granites: from segregation of melts to emplacement fabrics.* Kluwer, Dordrecht, 95-112.

BOUILLIN, J.-P., BOUCHEZ, J.-L., LESPINASSE, P. & PECHER, A. 1993. Granite emplacement in an extensional setting; an AMS study of the magmatic structures of Monte Capanne (Elba, Italy). *Earth and Planetary Science Letters,* 118, 263-279.

BUNGER, A. P. & CRUDEN, A. R. 2011. Modeling the growth of laccoliths and large mafic sills: Role of magma body forces. *Journal of Geophysical Research,* 116, B02203.

CALLOT, J. P. & GUICHET, X. 2003. Rock texture and magnetic lineation in dykes: a simple analytical model. *Tectonophysics,* 366, 207-222.

CORREA-GOMES, L. C., SOUZA FILHO, C. R., MARTINS, C. J. F. N. & OLIVEIRA, E. P. 2001. Development of symmetrical and asymmetrical fabrics in sheet-like igneous bodies: the role of magma flow and wall-rock displacements in theoretical and natural cases. *Journal of Structural Geology,* 23, 1415-1428.

CORRY, C. E. 1988. Laccoliths - Mechanics of emplacement and growth. *Geological Society of America Special Paper 220*, 110.

COTTAM, M., HALL, R., SPERBER, C. & ARMSTRONG, R. 2010. Pulsed emplacement of the Mount Kinabalu granite, northern Borneo. *Journal of the Geological Society,* 167, 49-60.

CRUDEN, A. R. & MCCAFFREY, K. J. W. 2001. Growth of plutons by floor subsidence: implications for rates of emplacement, intrusion spacing and melt-extraction mechanisms. *Physics and Chemistry of the Earth (A),* 26, 303-315.

DANIEL, J.-M. & JOLIVET, L. 1995. Detachment faults and pluton emplacement: Elba Island (Tyrrhenian Sea). *Bulletin de la Societé Géologique de France,* 166, 341-354.

Darrozes, J., Moisy, M., Olivier, P., Améglio, L. & Bouchez, J.-L. 1994. Structure magmatique du granite du Sidobre (Tarn, France): de l'echelle du massif à celle de echantillon. *Comptes Rendus de l'Académie des Sciences, paris,* 318, 243-250.

Dini, A., Corretti, A., Innocenti, F., Rocchi, S. & Westerman, D. S. 2007. Sooty sweat stains or tourmaline spots? The Argonauts on the Island of Elba (Tuscany) and the spread of Greek trading in the Mediterranean Sea. *In:* Piccardi, L. & Masse, W. B. (eds.) *Myth and Geology.* Geological Society, Special Publications, 273, London, 227-243.

Dini, A., Innocenti, F., Rocchi, S., Tonarini, S. & Westerman, D. S. 2002. The magmatic evolution of the laccolith-pluton-dyke complex of Elba Island, Italy. *Geological Magazine,* 139, 257-279.

Dini, A., Innocenti, F., Rocchi, S. & Westerman, D. S. 2006. The Late Miocene Christmas-tree laccolith complex of the Island of Elba, Italy. *In:* Pasquarè, G.*, et al.* (eds.) *Mapping Geology in Italy.* SELCA, Firenze, 249-258.

Dini, A., Westerman, D. S., Innnocenti, F. & Rocchi, S. 2008. Magma emplacement in a transfer zone: the Miocene mafic Orano dyke swarm of Elba Island (Tuscany). *In:* Thomson, K. & Petford, N. (eds.) *Structure and Emplacement of High-Level Magmatic Systems.* Geological Society, London, Special Publication 302, 131-148.

Dragoni, M., Lanza, R. & Tallarico, A. 1997. Magnetic anisotropy produced by magma flow: theoretical model and experimental data from Ferrar dolerite sills (Antarctica). *Geophysical Journal International,* 128, 230-240.

Farina, F., Dini, A., Innocenti, F., Rocchi, S. & Westerman, D. S. 2010. Rapid incremental assembly of the Monte Capanne pluton (Elba Island, Tuscany) by downward stacking of magma sheets. *Geological Society of America Bulletin,* 122, 1463-1479.

Geoffroy, L., Callot, J. P., Aubourg, C. & Moreira, M. 2002. Magnetic and plagioclase linear fabric discrepancy in dykes: a new way to define the flow vector using magnetic foliation. *Terra Nova,* 14, 183-190.

Gil-Imaz, A., Pocoví, A., Lago, M., Galé, C., Arranz, E., Rillo, C. & Guerrero, E. 2006. Magma flow and thermal contraction fabric in tabular intrusions inferred from AMS analysis. A case study in a late-Variscan folded sill of the Albarracín Massif (southeastern Iberian Chain, Spain). *Journal of Structural Geology,* 28, 641-653.

Guillet, P., Bouchez, J.-L. & Wagner, J. J. 1983. Anisotropy of magnetic susceptibility and magnetic structures in the Guérande granite massif (France). *Tectonics,* 2, 419-429.

Horsman, E., Tikoff, B. & Morgan, S. 2005. Emplacement-related fabric and multiple sheets in the Maiden Creek sill, Henry Mountains, Utah, USA. *Journal of Structural Geology,* 27, 1426-1444, doi:10.1016/j.jsg.2005.03.003.

Jelinek, V. 1981. Characterization of the magnetic fabric of rocks. *Tectonophysics,* 79, T63-T67.

Knight, M. D. & Walker, G. P. L. 1988. Magma flow directions in dikes of the Koolau Complex, Oahu, determined from magnetic fabric studies. *Journal of Geophysical Research: Solid Earth,* 93, 4301-4319.

KOMAR, P. D. 1972. Flow differentiation in igneous dykes and sills: profiles of velocity and phenocrysts concentration. *Geological Society of America Bulletin,* 83, 3443-3448.

KOMAR, P. D. 1976. Phenocryst interactions and the velocity profile of magma flowing through dykes and sills. *Geological Society of America Bulletin,* 87, 1336-1342.

KRATINOVÁ, Z., ZÁVADA, P., HROUDA, F. & SCHULMANN, K. 2006. Non-scaled analogue modelling of AMS development during viscous flow: A simulation on diapir-like structures. *Tectonophysics,* 418, 51-61.

LEUTHOLD, J., MÜNTENER, O., BAUMGARTNER, L. P., PUTLITZ, B., OVTCHAROVA, M. & SCHALTEGGER, U. 2012. Time resolved construction of a bimodal laccolith (Torres del Paine, Patagonia). *Earth and Planetary Science Letters,* 325–326, 85-92.

MAINERI, C., BENVENUTI, M., COSTAGLIOLA, P., DINI, A., LATTANZI, P., RUGGIERI, C. & VILLA, I. M. 2003. Sericitic alteration at the La Crocetta mine (Elba Island, Italy): interplay between magmatism, tectonics, and hydrothermal actvity. *Mineralium Deposita,* 38, 67-86.

MCCAFFREY, K. J. W. & PETFORD, N. 1997. Are granitic intrusion scale invariant? *Journal of the Geological Society, London,* 154, 1-4.

MENAND, T. 2008. The mechanics and dynamics of sills in layered elastic rocks and their implications for the growth of laccoliths and other igneous complexes. *Earth and Planetary Science Letters,* 267, 93-99.

MICHAUT, C. 2011. Dynamics of magmatic intrusions in the upper crust: Theory and applications to laccoliths on Earth and the Moon. *Journal of Geophysical Research: Solid Earth,* 116, B05205.

MICHEL, J., BAUMGARTNER, L., PUTLITZ, B., SCHALTEGGER, U. & OVTCHAROVA, M. 2008. Incremental growth of the Patagonian Torres del Paine laccolith over 90 k.y. *Geology,* 36, 459-462.

MILLER, C. F. & MILLER, J. S. 2002. Contrasting stratified plutons exposed in tilt blocks, Eldorado Mountains, Colorado River Rift, NV, USA. *Lithos,* 61, 209-224.

MILLS, R. D., RATNER, J. J. & GLAZNER, A. F. 2011. Experimental evidence for crystal coarsening and fabric development during temperature cycling. *Geology,* 39, 1139-1142.

MORGAN, S., STANIK, A., HORSMAN, E., TIKOFF, B., DE SAINT BLANQUAT, M. & HABERT, G. 2008. Emplacement of multiple magma sheets and wall rock deformation: Trachyte Mesa intrusion, Henry Mountains, Utah. *Journal of Structural Geology,* 30, 491-512.

O'DRISCOLL, B., STEVENSON, C. T. E. & TROLL, V. R. 2008. Mineral Lamination Development in Layered Gabbros of the British Palaeogene Igneous Province: A Combined Anisotropy of Magnetic Susceptibility, Quantitative Textural and Mineral Chemistry Study. *Journal of Petrology,* 49, 1187-1221.

PATERSON, S. R., FOWLER, T. K. J., SCHMIDT, K. L., YOSHINOBU, A. S., YUAN, E. S. & MILLER, R. B. 1998. Interpreting magmatic fabric patterns in plutons. *Lithos,* 44, 53-82.

PERTUSATI, P. C., RAGGI, G., RICCI, C. A., DURANTI, S. & PALMERI, R. 1993. Evoluzione post-collisionale dell'Elba centro-orientale. *Memorie della Società Geologica Italiana,* 49, 297-312.

ROCCHI, S., WESTERMAN, D. S., DINI, A. & FARINA, F. 2010. Intrusive sheets and sheeted intrusions at Elba Island (Italy). *Geosphere,* 6, 225-236.

ROCCHI, S., WESTERMAN, D. S., DINI, A., INNOCENTI, F. & TONARINI, S. 2002. Two-stage laccolith growth at Elba Island (Italy). *Geology,* 30, 983-986.

ROCHETTE, P., AUBOURG, C. & PERRIN, M. 1999. Is this magnetic fabric normal? A review and case studies in volcanic formations. *Tectonophysics,* 307, 219-234.

ROCHETTE, P., JACKSON, M. & AUBOURG, C. 1992. Rock magnetism and the interpretation of the anisotropy of magnetic susceptibility. *Reviews of Geophysics,* 30, 209-226.

ROCHETTE, P., JENATTON, L., DUPUY, C., BOUDIER, F. & REUBER, I. 1991. Emplacement modes of basaltic dykes in the Oman ophiolite: evidence from magnetic anisotropy with reference to geochemical studies. *In:* Peters, T. J. (ed.) *Ophiolite Genesis and the Evolution of the Oceanic Lithosphere.* Kluwer, Dordrecht, 55-82.

SAINT-BLANQUAT, M. D., HABERT, G., HORSMAN, E., MORGAN, S. S., TIKOFF, B., LAUNEAU, P. & GLEIZES, G. 2006. Mechanisms and duration of non-tectonically assisted magma emplacement in the upper crust: The Black Mesa pluton, Henry Mountains, Utah. *Tectonophysics,* 428, 1-31.

SAINT-BLANQUAT, M. D., LAW, R. D., BOUCHEZ, J.-L. & MORGAN, S. S. 2001. Internal structure and emplacement of the Papoose Flat pluton: An integrated structural, petrographic, and magnetic susceptibility study. *Geological Society of America Bulletin,* 113, 976-995.

SERRI, G., INNNOCENTI, F. & MANETTI, P. 2001. Magmatism from Mesozoic to Present: petrogenesis, time-space distribution and geodynamic implications. *In:* Vai, G. B. & Martini, I. P. (eds.) *Anatomy of an orogen: the Apennines and adjacent Mediterranean Basins.* Kluwer Academic Publisher, 77-104.

SERRI, G., INNOCENTI, F. & MANETTI, P. 1993. Geochemical and petrological evidence of the subduction of delaminated Adriatic continental lithosphere in the genesis of the Neogene-Quaternary magmatism of central Italy. *Tectonophysics,* 223, 117-147.

STEVENSON, C. T. E., OWENS, W. H. & HUTTON, D. H. W. 2007. Flow lobes in granite: The determination of magma flow direction in the Trawenagh Bay Granite, northwestern Ireland, using anisotropy of magnetic susceptibility. *Geological Society of America Bulletin,* 119, 1368-1386.

TARLING, D. H. & HROUDA, F. 1993. *The Magnetic Anisotropy of Rocks.* ed.).Chapman & Hall, London, 217.

TREVISAN, L. 1950. L'Elba orientale e la sua tettonica di scivolamento per gravità. *Memorie dell' Istituto di Geologia dell'Università di Padova,* 16, 1-30.

WESTERMAN, D. S., DINI, A., INNOCENTI, F. & ROCCHI, S. 2004. Rise and fall of a nested Christmas-tree laccolith complex, Elba Island, Italy. *In:* Breitkreuz, C. & Petford, N. (eds.) *Physical Geology of High-Level Magmatic Systems.* Geological Society, London, Special Publication 234, 195-213.

Table 1. *Angles between AMS data and megacrysts measurements*

			Foliation			
AMS station	Strike	Dip	Megacryst station	Strike	Dip	**Angle**
SM-BAR2	231.7	64.1	BardellaInf2	199	20	**48**
SM-CBAL2	142.7	23.3	Napoleone	*158*	38	**17**
SM-CI1A	30.5	42.2	CasaIschia6a	60	50	**22**
SM-CI1B	62.8	53.1	CasaIschia6b	78	49	**17**
SM-CI1C	52.5	69.3	CasaIschia6c	74	64	**20**
SM-CI5	324.0	23	CasaIschia3/4	94	5	**33**
SM-CI4	51.0	44	CasaIschia5	45.6	42.7	**7**
SM-CI3	264.8	66.3	CasaIschia1	291	49	**29**
SM-CI6	247.0	64.0	CasaIschia2	20	46	**48**
SM-CI9c	229.0	3.0	CasaIschia0a	329	11	**13**
SM-DWF3	151.7	84.8	DykeWFonza	321	78	**20**
SM-ENF34	69	82	ViticcioNorth	53	69	**26**
SM-ENF4	59.0	61.7	ViticcioStreet	231	89	**28**
SM-ENF53	351	40	ViticcioSouth	15	25	**19**
SM-FOR2b	231.2	38.1	Forno2	208	58	**26**
SM-LAM6	289.0	86.0	Lamaia2	261	25	**72**
SM-LAM1	308.1	14.3	Lamaia3	286	16	**6**
SM-LAM10	264.3	56.3	Lamaia6	235	33	**29**
SM-LAM12	253.7	36.8	Lamaia8	242	35	**7**
SM-LAM2	254.9	54.3	Lamaia5	241	30	**26**
SM-LAM3B	253.4	24.8	Lamaia9	270	19	**8**

SM-LAM4	84.7	69.1	Lamaia1	238	20	**87**
SM-LAM9	240.4	59.6	Lamaia6	225	49	**16**
SM-PM1	156.4	34.2	PuntaMele1	206	27	**52**
SM-PM2	338.0	75.9	PuntaMele2	163	32	**72**
% of stations where angle between two datasets is < 30°:						**71**

Lineation

AMS station	Bearing	Plunge	Megacryst station	Bearing	Plunge	**Angle**
SM-ENF4	71.5	21.8	Viticcio street	227	12	**40**
SM-LAM9	55.5	8.2	Lamaia6	26	21	**29**
SM-LAM10	43.7	44.3	Lamaia7	29	18	**28**
SM-CI3	62.8	40.4	CasaIschia1	74	36	**10**
SM-PM1	328.3	5.5	PuntaMele1	354	11	**27**
SM-BAR1	293.6	27.8	BardellaInf1	314	14	**23**
% of stations where angle between two datasets is < 30°:						**83**

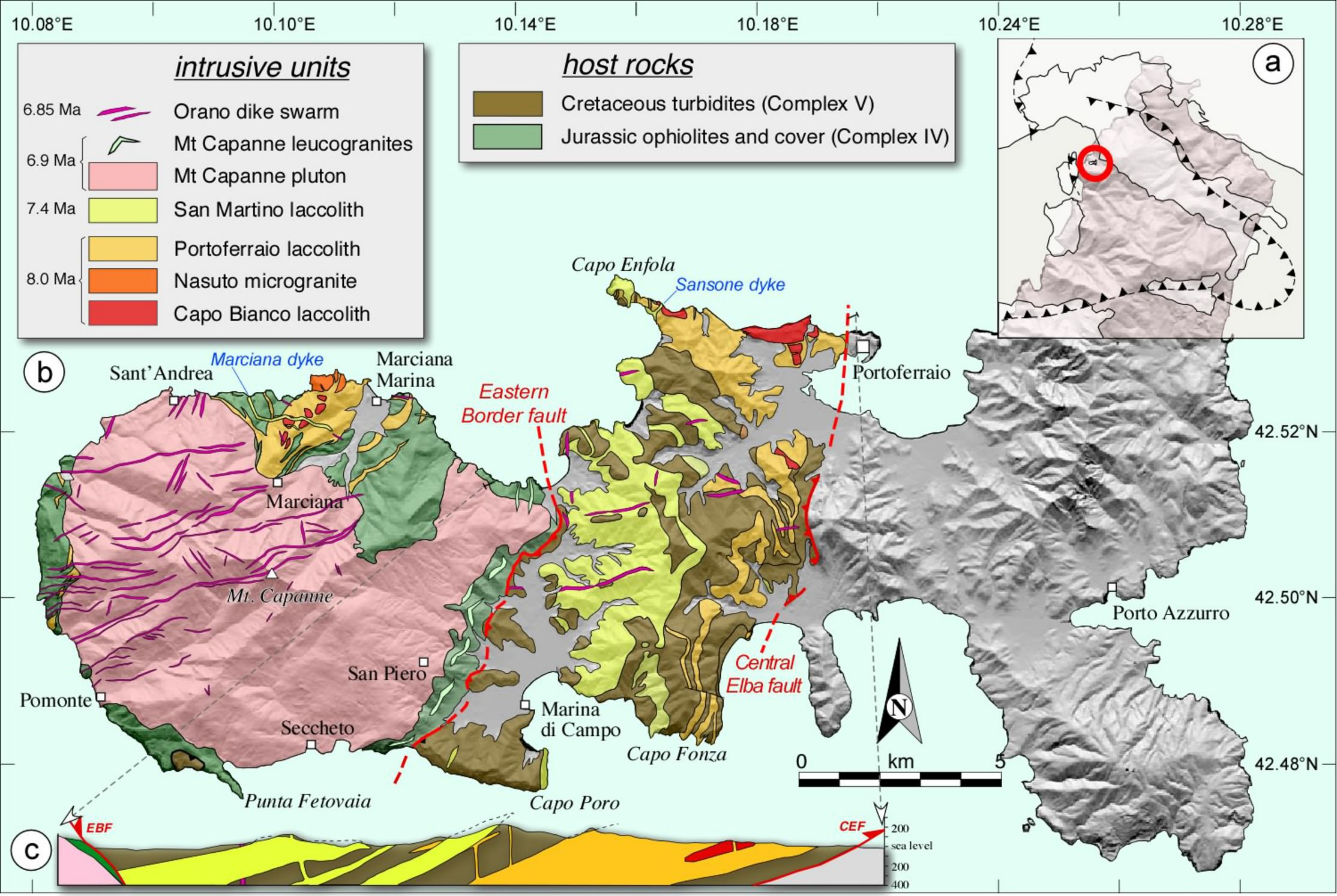
10.08°E
10.10°E
10.14°E
10.18°E
10.24°E
10.28°E
intrusive units
6.85 Ma
Orano dike swarm
6.9 Ma
Mt Capanne leucogranites
Mt Capanne pluton
7.4 Ma
San Martino laccolith
8.0 Ma
Portoferraio laccolith
Nasuto microgranite
Capo Bianco laccolith
host rocks
Cretaceous turbidites (Complex V)
Jurassic ophiolites and cover (Complex IV)
a
b
c
Capo Enfola
Sansone dyke
Marciana dyke
Sant'Andrea
Marciana Marina
Eastern Border fault
Portoferraio
Marciana
Mt. Capanne
Central Elba fault
Porto Azzurro
San Piero
Pomonte
Marina di Campo
Secchetto
Capo Fonza
Punta Fetovaia
Capo Poro
N
0
km
5
42.52°N
42.50°N
42.48°N
EBF
CEF
200
sea level
200
400

Figure 1

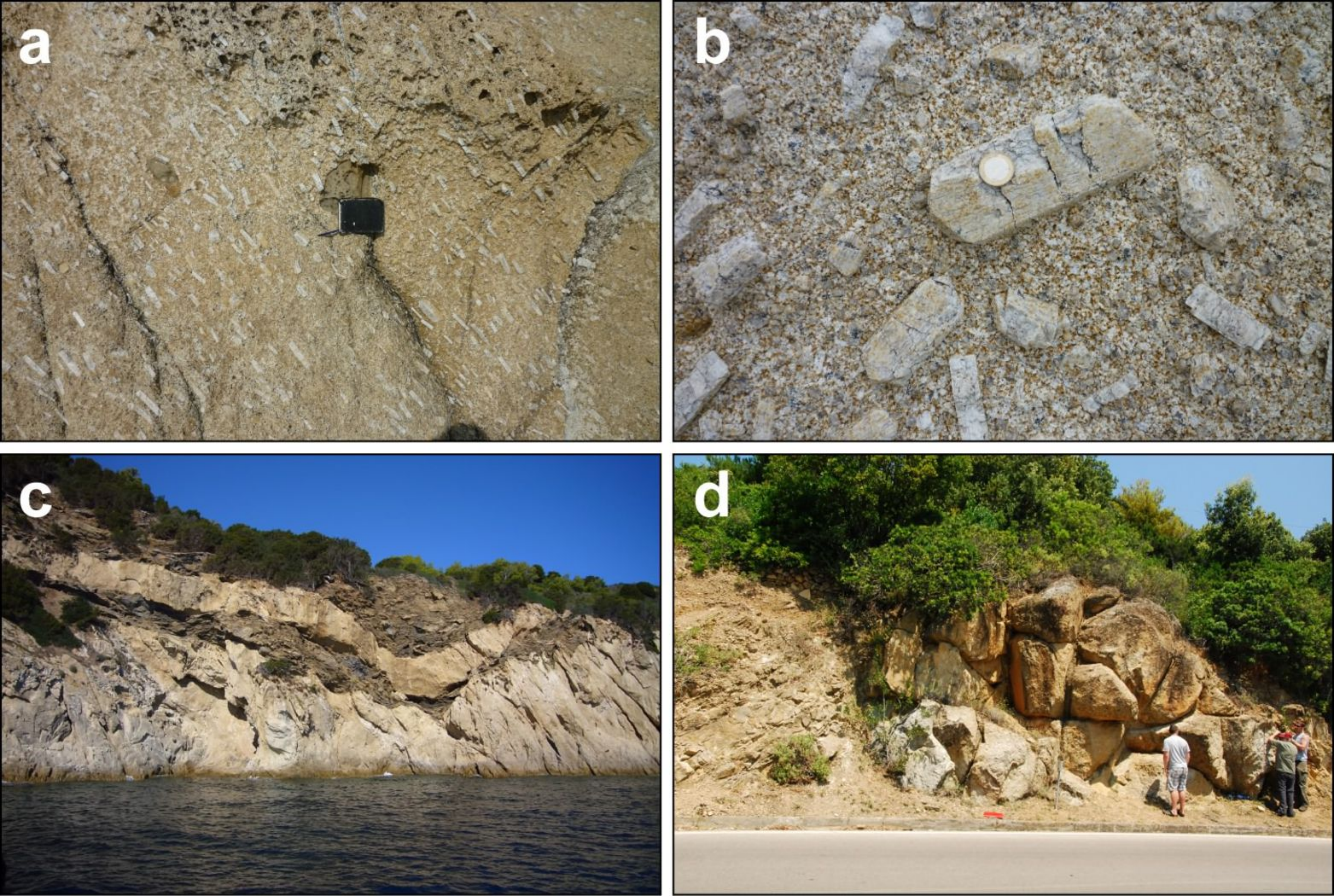
a
b
c
d

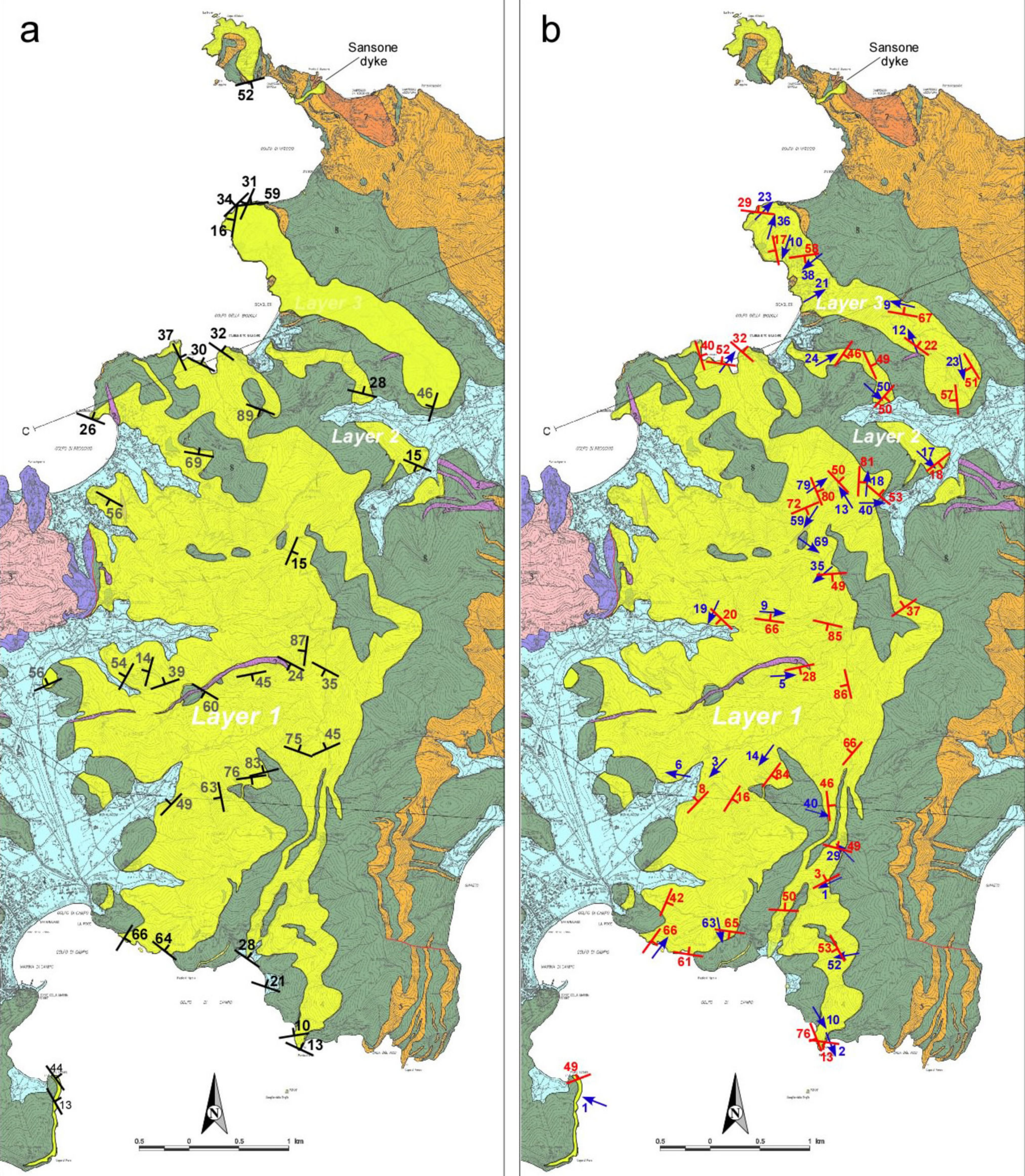
a
Sansone dyke
Layer 3
Layer 2
Layer 1
C
0.5 0 0.5 1 km
N
b
Sansone dyke
Layer 3
Layer 2
Layer 1
C
0.5 0 0.5 1 km
N

a
0.2 mm
b
anatase
titanite
0.2 mm
c
d
e
heating
cooling
Total uncorrected susceptibility
Temperature
-90
-100
-110
-120
-130
-140
-150
0
100
200
300
400
500
600
700

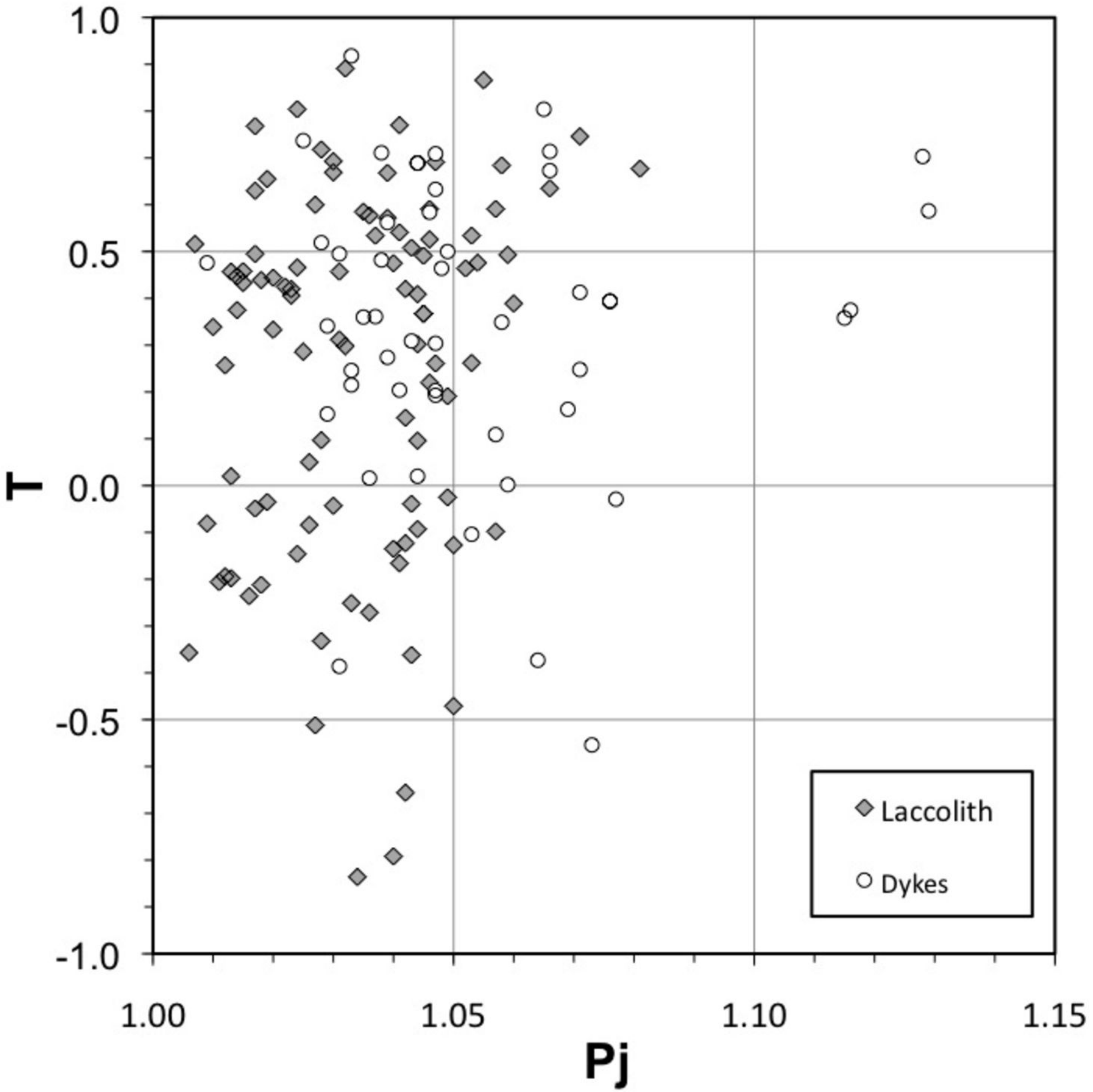

1.0
0.5
0.0
-0.5
-1.0
T
1.00
1.05
1.10
1.15
Pj
Laccolith
Dykes

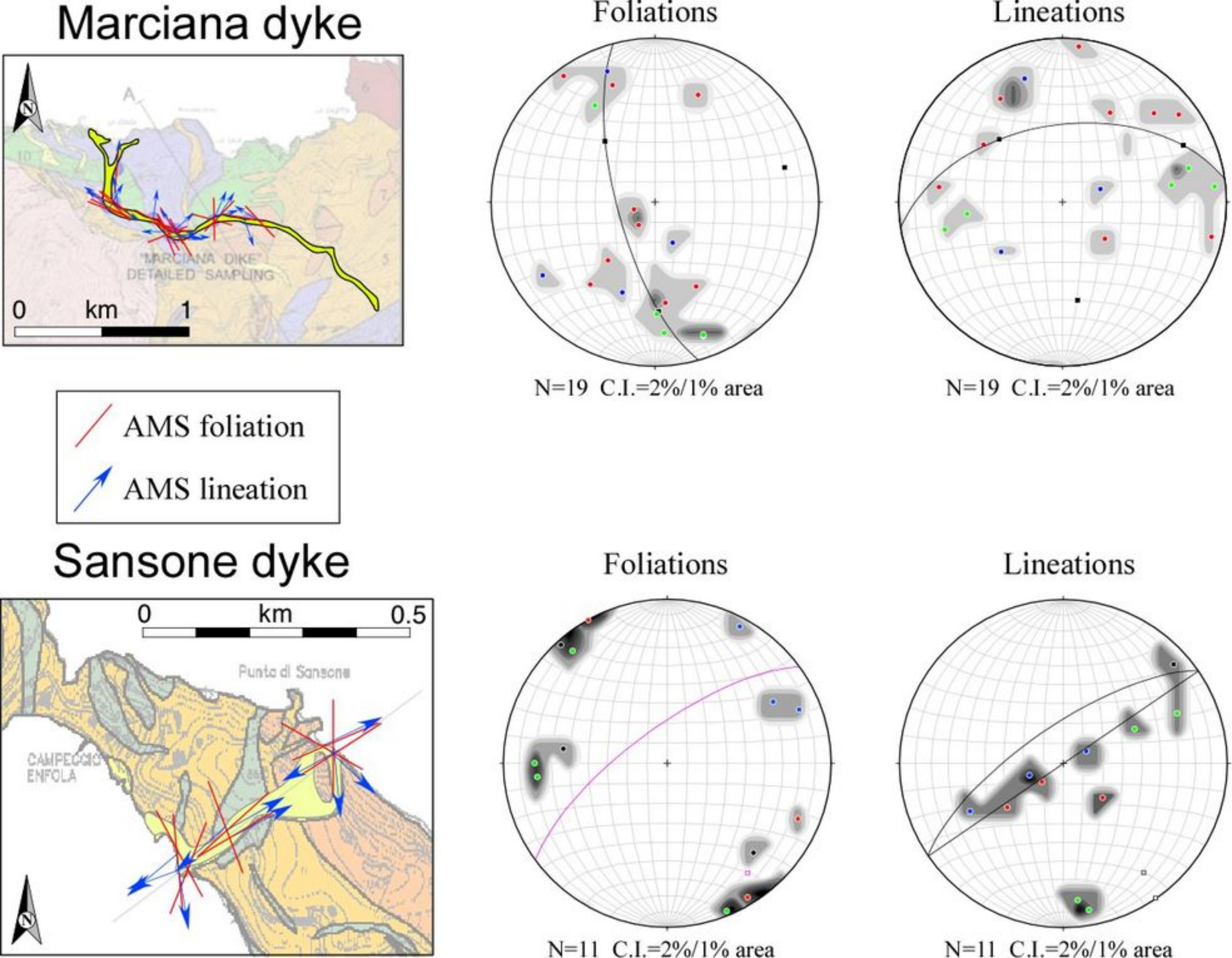

Marciana dyke
"MARCIANA DIKE"
DETAILED SAMPLING
0
km
1
Foliations
N=19 C.I.=2%/1% area
Lineations
N=19 C.I.=2%/1% area
AMS foliation
AMS lineation
Sansone dyke
0
km
0.5
Punta di Sansone
Foliations
N=11 C.I.=2%/1% area
Lineations
N=11 C.I.=2%/1% area


upward flow
downward flow
Pole to K-feldspar foliation
dip = 0 - 29°
dip = 30 - 59°
dip = 60 - 90°
multiple crystal measurements e > 25
multiple crystal measurements e < 25
field observation
Pole to AMS foliation
dip = 0 - 29°
dip = 30 - 59°
dip = 60 - 90°
average K3 orientation e > 25
average K3 orientation e < 25
0.5
0
0.5
1 km